ANTIOXIDANTS & REDOX SIGNALING
Volume 20, Number 7, 2014

DOI: 10.1089/ars.2013.5292

Discoveries

ORIGINAL RESEARCH COMMUNICATION

miR-205 Hinders the Malignant Interplay Between Prostate Cancer Cells and Associated Fibroblasts

Paolo Gandellini,[1,*] Elisa Giannoni,[2,*] Anna Casamichele,[1] Maria Letizia Taddei,[2] Maurizio Callari,[1] Claudia Piovan,[1,3] Riccardo Valdagni,[4,5] Marco Alessandro Pierotti,[6] Nadia Zaffaroni,[1,*] and Paola Chiarugi[2,*]

Abstract

Aims: Tumor microenvironment is a strong determinant for the acquisition of metastatic potential of cancer cells. We have recently demonstrated that cancer-associated fibroblasts (CAFs) elicit a redox-dependent epithelial-mesenchymal transition (EMT) in prostate cancer (PCa) cells, driven by cycloxygenase-2/hypoxia-inducible factor-1 (HIF-1)/nuclear factor-κB pathway and enhancing tumor aggressiveness. Here, we investigated the involvement of microRNAs (miRNAs) in tumor-stroma interplay to identify possible tools to counteract oxidative stress and metastasis dissemination. ***Results:*** We found that *miR-205* is the most downmodulated miRNA in PCa cells upon CAF stimulation, due to direct transcriptional repression by HIF-1, a known redox-sensitive transcription factor. Rescue experiments demonstrated that ectopic *miR-205* overexpression in PCa cells counteracts CAF-induced EMT, thus impairing enhancement of cell invasion, acquisition of stem cell traits, tumorigenicity, and metastatic dissemination. In addition, *miR-205* blocks tumor-driven activation of surrounding fibroblasts by reducing pro-inflammatory cytokine secretion. ***Innovation:*** Overall, such findings suggest *miR-205* as a brake against PCa metastasis by blocking both the afferent and efferent arms of the circuit between tumor cells and associated fibroblasts, thus interrupting the pro-oxidant and pro-inflammatory circuitries engaged by reactive stroma. ***Conclusion:*** The evidence that *miR-205* replacement in PCa cells is able not only to prevent but also to revert the oxidative/pro-inflammatory axis leading to EMT induced by CAFs sets the rationale for developing miRNA-based approaches to prevent and treat metastatic disease. *Antioxid. Redox Signal.* 20, 1045–1059.

Introduction

Mounting evidence supports the notion that progression of aggressive carcinoma is strongly influenced by microenvironmental cues, including hypoxia, acidity, composition of extracellular matrix (ECM), and host stromal cells, collectively called "reactive stroma" (26,53). Among stromal cells, cancer-associated fibroblasts (CAFs), either resident or recruited from circulating bone marrow-derived mesenchymal cells, have been reported to play a key role in malignant progression (4,5,12,29). Indeed, they act through secretion of soluble growth factors and inflammatory cytokines, production of ECM proteins, and release of matrix metalloproteases (MMPs) (12,23). Moreover, CAFs engage a bidirectional interplay with cancer cells, acting on them through the so-called "efferent way," thereby enhancing their malignancy (14). However, they are themselves sensitive to factors released by cancer cells and undergo a differentiation process called mesenchymal-mesenchymal transition (11,29), converting them into reactive CAFs, a phenotype similar to myofibroblasts (27,47,55).

[1]Department of Experimental Oncology, [4]Department of Radiotherapy, [5]Prostate Program, and [6]Scientific Directorate, Fondazione IRCCS Istituto Nazionale dei Tumori, Milan, Italy.
[2]Department of Experimental and Clinical Biomedical Sciences, University of Florence, Florence, Italy.
[3]Departments of Molecular Virology, Immunology and Human Genetics, Comprehensive Cancer Center, Ohio State University, Columbus, Ohio.
*These authors equally contributed to the work.

Innovation

Epithelial-mesenchymal transition (EMT), a motogen and redox-dependent program used by cancer cells to escape the hostile primary tumor milieu, is engaged in response to activation of cancer-associated fibroblasts (CAFs) and/or incipient hypoxia. Here, we identify *miR-205* as a mandatory molecular player of CAF-driven EMT, acting downstream to cycloxygenase-2-mediated oxidative stress and stabilization of hypoxia-inducible factor-1α and affecting stemness of metastatic cells. Noteworthy, ectopic overexpression of *miR-205* can both prevent and rescue stromal reactivity and cancer aggressiveness, in addition to survival and growth of metastatic colonies, thereby representing a novel and promising tool for therapeutic approaches aimed at regulating epithelial/mesenchymal cell plasticity.

In addition to tumor growth factor-β (TGF-β), we recently acknowledged interleukin-6 (IL-6) as the main factor secreted by aggressive prostate cancer (PCa) cells, which elicits reactivity of stromal fibroblasts and converts them into CAFs (23). In turn, activated CAFs secrete MMP-2 and MMP-9, which induce epithelial-mesenchymal transition (EMT) in PCa cells, thus ultimately enhancing their aggressiveness (18,23). Indeed, EMT has been associated with increase in proteolytic motility of cancer cells, enhancement of anoikis resistance, and achievement of stem-like traits (7,24,34). In keeping with such observations, PCa cells experiencing EMT upon CAF contact enhance their invasiveness, self-renewal ability, capacity to grow as adherence-independent prostaspheres, expression of stemness markers, and ability to spread as spontaneous lung metastases. CAF-induced EMT of PCa cells is driven by a pro-oxidant pathway involving activation of Rac1b and leading to delivery of reactive oxygen species (ROS), through the modulation of cycloxygenase-2 (COX-2) (22,50). Oxidative stress leads to activation of two redox-sensitive transcription factors, hypoxia-inducible factor-1α (HIF-1α) and nuclear factor-κB (NF-κB), which start the EMT transcriptional program (22,40,46).

We identify in microRNAs (miRNAs), endogenous small non-coding RNAs that negatively regulate gene expression during key cellular processes (2), potential candidate mediators of CAF-induced EMT. A few miRNAs have been involved in ROS handling by cancer cells and in EMT regulation. For example, members of the *miR-200* family have been shown to regulate EMT through the control of key transcription factors like ZEBs and Snails (25,28,37,56), although a direct regulation by elements of the tumor microenvironment has not been reported. In addition, *miR-141* and *miR-200a* have been involved in Nrf2/Keap1 oxidative stress and response to paclitaxel therapy of ovarian cancers (36).

The aim of this study was to identify miRNAs specifically involved in EMT engaged by CAFs in PCa cells and establish their hierarchy with the already accredited signaling pathways involving redox regulation of HIF-1α and NF-κB, to develop possible tools to target EMT and prevent metastasis dissemination.

Results

miR-205 is repressed in PC-3 cells upon CAF stimulation

To verify whether specific miRNAs are involved in CAF-induced EMT in PCa cells, PC-3 cells were subjected to a variety of stimuli [known to induce or not the acquisition of a mesenchymal phenotype (22,23)] and profiled for miRNA expression on a microarray platform. Unsupervised hierarchical clustering showed that miRNA profiles could distinguish cells that underwent EMT following stimulation with activated fibroblasts (including CAFs and human prostate fibroblasts—here referred to as HPFs—activated *in vitro* with IL-6 or TGF-β) from cells that did not, such as unstimulated or HPF-stimulated cells (Fig. 1A). PC-3 cells pre-incubated with siRNA against HIF-1α or COX-2 (assessment of their knockdown is reported in Supplementary Fig. S1; Supplementary Data are available online at www.liebertpub.com/ars), leading players of the pro-inflammatory signature engaged in cancer cells by CAFs (22), segregated with controls, irrespective of CAF stimulation (Fig. 1A). When a class comparison was applied to cells undergoing or not CAF-induced EMT, 28 miRNAs were found to be significantly (P-value < 0.0001) differentially expressed, with a higher proportion of downregulated miRNAs in mesenchymal cells (Fig. 1A and Supplementary Table S1). This can be partially explained by the reduction of Drosha expression levels observed in PC-3 cells stimulated with activated fibroblasts (Supplementary Fig. S2), which may account for impaired processing of miRNAs from their primary transcripts. Notably, Dicer expression resulted to be unaffected (Supplementary Fig. S2) and, in any case, intervention of additional mechanisms must be envisaged to explain CAF-induced upmodulation or repression of specific miRNAs, including transcriptional regulation. Among downregulated miRNAs we found members of *miR-200* family, already reported to negatively regulate TGF-β-induced EMT (25), and *miR-205*, which we previously showed to counteract EMT in PCa cells (19) (Fig. 1A and Supplementary Table S1). Specifically, *miR-205* appeared to be the most downmodulated miRNA in PC-3 cells exposed to CAFs (Fig. 1A and Supplementary Table S1), as also confirmed by quantitative reverse transcriptase-polymerase chain reaction (qRT-PCR) (Fig. 1B). Again, the RNA interference with COX-2 or HIF-1α led to almost complete abolishment of *miR-205* and *miR-200b* downmodulation (Fig. 1B).

miR-205 loss is associated with PCa progression and metastasis

Downregulation of *miR-205* in PCa compared to normal tissues was initially reported by us (19) and confirmed later by a number of miRNA expression profiling studies [reviewed in Gandellini *et al.* (20)]. To specifically assess the impact of *miR-205* downmodulation on PCa progression and metastasis, we analyzed the largest available set of miRNA and gene expression profiling data (52). *MiR-205* expression levels were globally reduced in primary carcinomas compared with normal tissues and further diminished in metastases (Fig. 2A). The miRNA level distribution across primary tumors, all obtained from treatment-naive patients subjected to radical prostatectomy, highlighted a subset of cases (about 17%) with

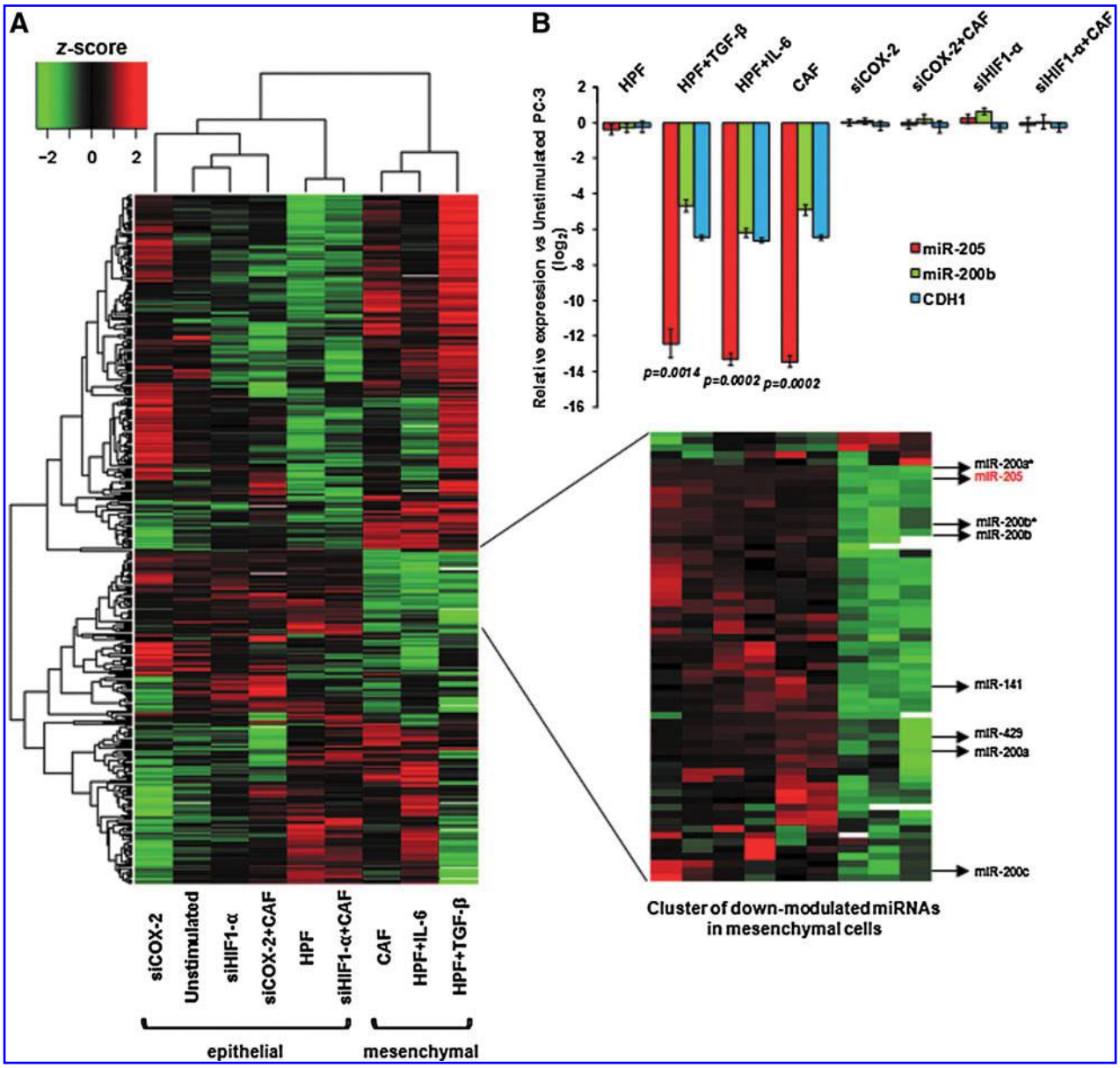

FIG. 1. ***miR-205* is downregulated in PCa cells stimulated with activated fibroblasts. (A)** Unsupervised hierarchical clustering analysis based on miRNA expression data of PC-3 cells subjected to a variety of stimuli. miRNA expression profiles successfully distinguished cells that underwent EMT following stimulation with activated fibroblasts (here referred to as "mesenchymal") from cells that did not ("epithelial"). A cluster of miRNAs downregulated in PC-3 cells undergoing CAF-induced EMT (including *miR-200* family members and *miR-205*) is highlighted on the right. **(B)** Quantitative reverse transcriptase-polymerase chain reaction measurement of *miR-205*, *miR-200b*, and E-cadherin (*CDH1*) expression levels in PC-3 cells subjected to different stimuli. Data are reported as $\log_2$-transformed relative quantity with respect to unstimulated cells and represent the mean ± standard deviation (SD) of three experiments. miRNA, microRNA; PCa, prostate cancer; EMT, epithelial-mesenchymal transition; CAF, cancer-associated fibroblast.

expression levels comparable to those of metastases (Fig. 2A, B). Strikingly, such cases derived from patients a significantly increased risk (hazard ratio, 0.28; 95% confidence limits, 0.1–0.77; *P*-value = 0.014) of experiencing biochemical relapse within 5 years (Fig. 2C).

To further elucidate the role of *miR-205* in PCa, gene set enrichment analysis (GSEA) was performed on genes correlated with *miR-205* expression in the aforementioned dataset. Among positively correlated genes, we found significant enrichment of gene sets reported to be down-modulated in PCa by different groups (Liu, Tomlins datasets) or downregulated in metastates (Jaeger, Chandran, Provenzani datasets) (Fig. 2D and Supplementary Table S2). Among negatively correlated genes were instead those upregulated in PCa (Liu, Tomlins, Wallace datasets), in metastases (Bidus dataset), or during EMT (Sarrio dataset), thus highlighting, in the clinical setting, the possible antagonistic effect of *miR-205* on the development and progression of the disease (Fig. 2D and Supplementary Table S3).

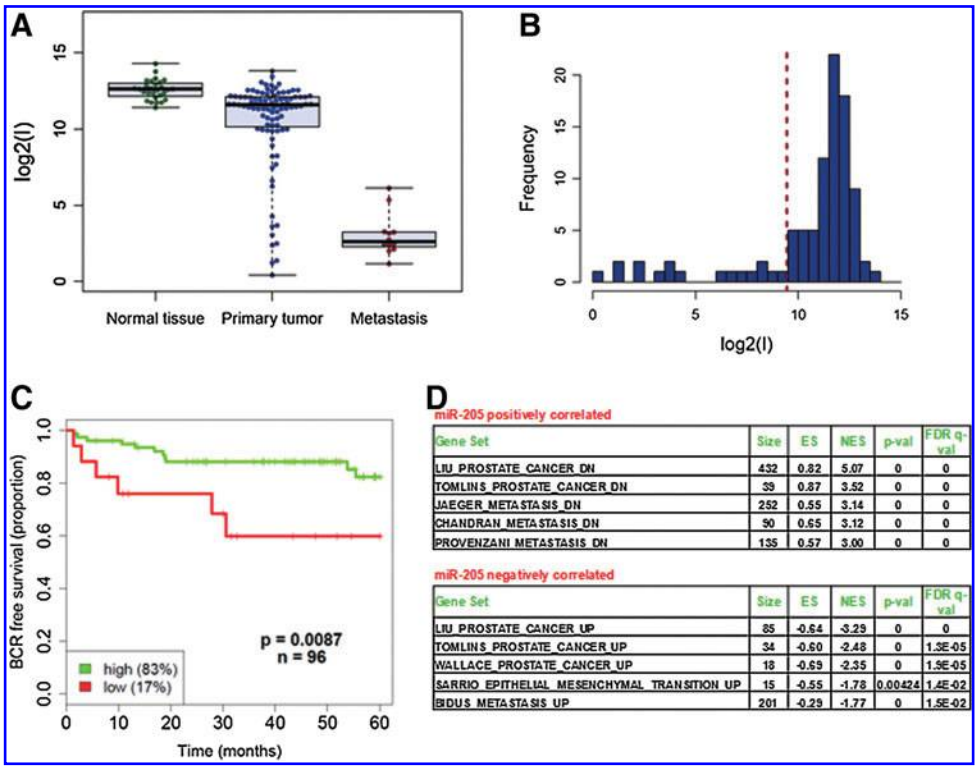

FIG. 2. ***miR-205* loss is associated with prostate cancer progression and metastasis. (A)** *miR-205* expression pattern was studied in normal prostate tissues ($n=28$), primary tumors ($n=96$), and metastatic lesions ($n=12$) from Taylor's dataset (GSE21032). Expression (here reported as $\log_2$-transformed value of microarray intensity, I) is significantly lower in primary tumors than in normal prostate (P-value $=0.0007$, modified t test) and further reduced in metastatic lesions (P-value $=7\times10^{-15}$, modified t test). **(B)** A skewed distribution in *miR-205* expression levels was observed in primary tumors, and "miR-low" and "miR-high" tumors were identified using the plotted threshold (dashed red line). **(C)** Kaplan–Meier curves showing a significant association between high or low *miR-205* expression and time to biochemical relapse (BCR). **(D)** Representative gene sets significantly enriched among genes positively or negatively correlated with *miR-205* expression in Taylor's dataset. Details and references of gene sets can be found at www.broadinstitute.org/gsea/msigdb/. To see this illustration in color, the reader is referred to the web version of this article at www.liebertpub.com/ars

A hierarchy exists between miR-205 downregulation and the proinflammatory pathway leading to EMT

To evaluate the kinetics of *miR-205* downmodulation induced by tumor stroma and to assess whether reduction of *miR-205* was either due to increased degradation or reduced transcription/processing, the levels of the primary transcript (pri-*miR-205*) and the mature form of the miRNA were measured at different time points after stimulation of PC-3 cells with CAF-conditioned medium (CM), obtained by treating CAFs with serum-free medium for 48 h. Serum-starved cells were used as control. We found that expression of both pri-*miR-205* and mature *miR-205* started to decrease from day 2 and returned to normal levels from day 5 (Fig. 3A), thus completely matching the derepression of *miR-205* direct targets ZEB1 and ZEB2 (Fig. 3A). Accordingly, overlap between *miR-205* reduction and appearance of EMT traits, such as downmodulation of E-cadherin and upregulation of vimentin, was observed (Fig. 3B). The expression of other EMT-related transcription factors (*i.e.*, *SNAI1*, *SNAI2*, and *TWIST1*) was not substantially modulated compared to changes in *miR-205*, *ZEB1*, and *ZEB2* (Supplementary Fig. S3). Notably, activation of HIF-1α, COX-2, and NF-κB pathways peaked at day 1 and became negligible from day 4 (Fig. 3B). Taken together, these data suggested that *miR-205* is mainly repressed at the transcriptional level, hypothesis strengthened by the observation that the expression levels of *miR-205* primary transcript are lowered despite potential reduced processing to pre-miRNA due to Drosha downregulation (Supplementary Fig. S2). In addition, HIF-1α and NF-κB may be potential direct transcriptional repressors, since their activation immediately precedes reduction of *miR-205* expression levels and modulation of ZEB1/2. Again, CAF-induced EMT appears reversible, likely due to depletion of specific factors produced by CAFs. Actually, reversion of EMT is accelerated by removing CAF-CM (Fig. 3C), suggesting that CAF-induced EMT is an epigenetic phenomenon that is not genetically fixed.

To assess whether *miR-205* is transcriptionally repressed by HIF-1α, which we have acknowledged to be redox-targeted by the COX-2-dependent EMT activation (22), its promoter (3) was scanned for potential binding sites. We found at least six highly predicted consensus sequences for the transcription factor, three of which on the sense strand (Fig. 4A). Chromatin immunoprecipitation (ChIP) experiments performed using primers to amplify regions containing the three sites (Fig. 4A) evidenced increased PCR signal for all the regions in anti-HIF-1α *versus* IgG immunoprecipitants from CAF-stimulated cells, especially for site 1 (132-fold increase), thus confirming enriched binding of HIF-1α to such consensus sequences

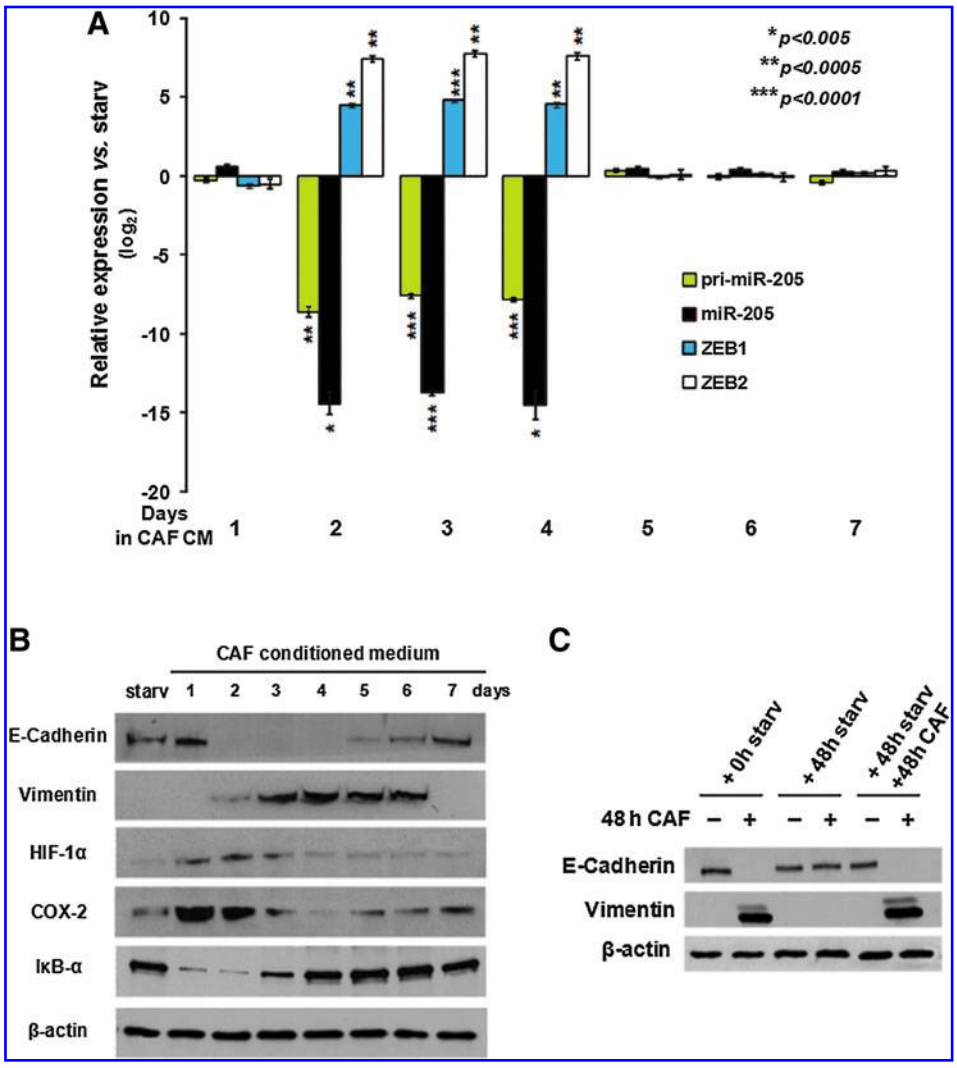

FIG. 3. CAF-induced proinflammatory signature correlates with *miR-205* transcriptional repression. (A) The expression of pri-*miR-205*, mature *miR-205*, *ZEB1*, and *ZEB2* was measured by quantitative reverse transcriptase-polymerase chain reaction in CAF-stimulated PC-3 cells at different time intervals. Data are reported as $\log_2$-transformed relative expression with respect to serum-starved cells (named Starv). **(B)** The levels of E-cadherin, vimentin, HIF-1α, COX-2, and IκB-α (the phosphorylation of which is inversely proportional to NF-κB activation) were assessed by immunoblotting in CAF-stimulated PC-3 cells. **(C)** PC-3 cells were either incubated with CM from CAFs (obtained from fibroblasts treated with serum-free medium for 48 h) or serum-starved for 48 h and subsequently (i) harvested (lanes 1, 2), (ii) serum-starved for additional 48 h (lanes 3, 4), or (iii) serum-starved for 48 h, then treated with starvation medium or CM from CAFs for additional 48 h (lanes 5, 6). E-cadherin and vimentin levels were evaluated on cell lysates. HIF-1α, hypoxia-inducible factor-1α; COX-2, cycloxygenase-2; NF-κB, nuclear factor-κB; CM, conditioned medium. To see this illustration in color, the reader is referred to the web version of this article at www.liebertpub.com/ars

(Fig. 4B, CAF lanes). All three regions appeared to be essentially unbound in HPF-stimulated cells but showed 7.7-, 3.2-, and 2.8-fold enriched binding, respectively, upon CAF stimulation (Fig. 4B). Such findings suggest that changes in HIF-1α steady-state levels, such as those deriving from CAF stimulation, may alter *miR-205* promoter occupancy by HIF-1α and, consequently, affect miRNA transcription. To further prove that *miR-205* is subjected to direct transcriptional repression, we obtained a plasmid containing a portion of 2 kb of *miR-205* promoter, which contains two of the three HIF-1α binding sites, cloned upstream to firefly luciferase (49). PC-3 cells were transfected for 4 h with such a construct, together with pRL-TK renilla luciferase vector, then stimulated with the CM from either CAFs or HPFs. Dual luciferase assay was then performed at different time points after transfection to calculate the firefly/renilla ratio. Results showed a significant decrease in the ratio in CAF-treated compared to HPF-treated cells at all time points considered (24, 48, and 72 h), suggesting that the 2 kb portion of *miR-205* promoter is directly responsive to factors produced by CAFs (Supplementary Fig. S4), such as HIF-1α.

In keeping with these data, culturing of PC-3 cells under hypoxic conditions, which also increase HIF-1α levels (Fig. 4C), caused a time-dependent downmodulation of both primary and mature *miR-205* transcripts (Fig. 4D). Interestingly, downmodulation of *miR-205* after HIF-1α activation by hypoxia again seemed to be a reversible phenomenon, as recovery of cells in normoxia restored or even increased the levels of primary and mature *miR-205* (Fig. 4D). Similar results were obtained by culturing cells in the presence of cobalt chloride ($CoCl_2$), which stabilizes HIF-1α protein by inhibiting prolyl hydroxylase activity (51), for different time intervals and recovering them in $CoCl_2$-free medium (Supplementary Fig. S5). Again, HIF-1α activation induced a reversible downregulation of pri-*miR-205* levels, which was, however, insufficient to induce robust modulations of mature *miR-205* within the experimental time frame (Supplementary Fig. S5).

miR-205 prevents CAF-induced EMT and fibroblast activation by PCa cells

To investigate whether *miR-205* downmodulation is functionally involved in CAF-induced EMT, a rescue experiment, where reduction of miRNA levels was prevented by transfecting PC-3 cells with synthetic *miR-205* precursor prior to

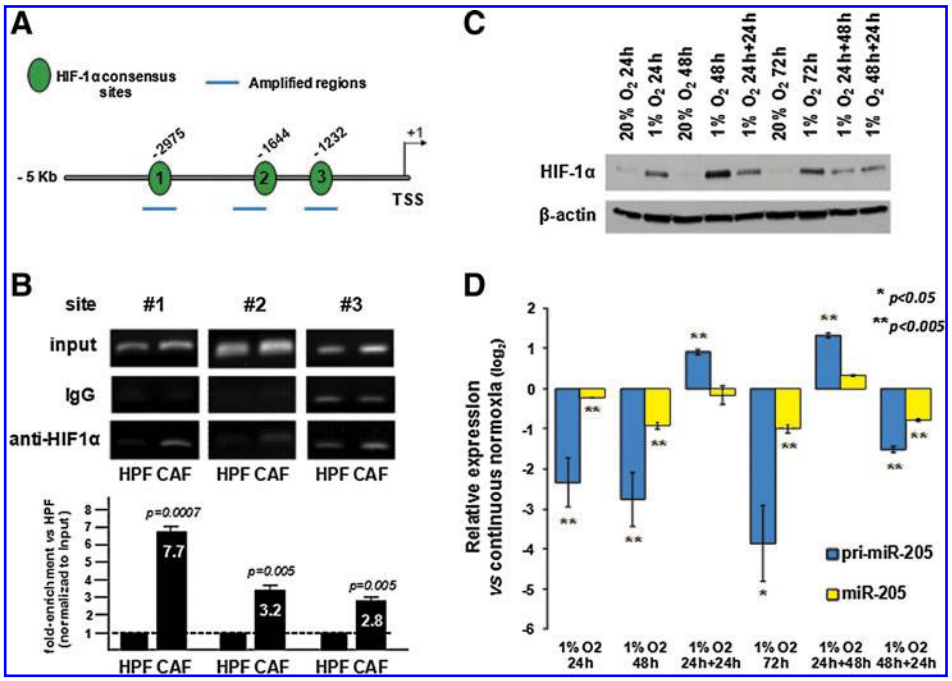

FIG. 4. HIF-1α directly represses *miR-205* transcription. (A) Representation of *miR-205* promoter, recently identified as the 5 kb sequence upstream of *miR-205* transcriptional start site (TSS) (3). Green ovals represent *in silico*-predicted HIF-1 binding sites. Light blue lines identify the regions amplified in chromatin immunoprecipitation experiments. **(B)** Chromatin from fibroblast-stimulated PC-3 cells was precipitated with anti-HIF-1α antibody, and then the regions putatively bound by HIF-1 were amplified by RT-PCR (*top*). Normal mouse preimmuned IgG was used as a negative control. Densitometric analysis of PCR signals in immunoprecipitants, reported as normalized to input DNA from each sample (*bottom*). Data are reported as mean ± SD of three experiments. **(C)** HIF-1α immunoblotting on PC-3 cells either cultivated in hypoxia (1% O_2) or normoxia (20% O_2) for the indicated time intervals (either continuously or with a hypoxia pulse followed by recovery in 20% oxygen atmosphere). **(D)** qRT-PCR assessment of pri-*miR-205* and mature *miR-205* expression in PC-3 cells cultured as in **(C)**. Data are reported as $\log_2$-transformed relative expression with respect to cells cultured in normoxic conditions and harvested at each time point (24, 48, and 72 h). qRT-PCR, quantitative reverse transcriptase-polymerase chain reaction. To see this illustration in color, the reader is referred to the web version of this article at www.liebertpub.com/ars

CAF stimulation, was carried out. Transfection efficiency was checked using a fluorescein-labeled oligomer and found to be ~90% after a 4-h transfection (Supplementary Fig. S6A). Moreover, transfection of PC-3 cells with synthetic miRNA precursor resulted in a marked overexpression (387- and 179-fold at days 1 and 2 post-transfection, respectively) of mature *miR-205*, as assessed by qRT-PCR (Supplementary Fig. S6B). Conspicuous overexpression of *miR-205* was found to persist in *miR-205*-transfected cells until 9 days after transfection, when a 17-fold overexpression of the miRNA was observed (Supplementary Fig. S6B).

Ectopic *miR-205* expression efficiently prevented loss of E-cadherin expression (Fig. 5A), attenuated the increase in cell invasion (Fig. 5B), and reduced *anoikis* resistance (Fig. 5C) of PC-3 cells stimulated with CAFs. Further, in keeping with the strict link between EMT and the achievement of stem-like traits (23,34,44), ectopic *miR-205* overexpression in PCa cells counteracted the acquisition of stem-like properties, in terms of prostasphere formation (Fig. 5D) and presence of $CD44^{high}/CD24^{low}$ (Fig. 5E) and CD133-positive subpopulations (Fig. 5F), acknowledged markers of PCa stem cells (8,31,48). Interestingly, silencing of the only *miR-205* in PC-3 cells by the use of locked nucleic acid (LNA)-modified antisense oligonucleotide phenocopied CAF-induced EMT, in terms of E-cadherin and Vimentin expression pattern, and the CAF-induced pro-invasive effect and acquisition of stem cell traits (Supplementary Fig. S7). Notably, the ability to undergo CAF-mediated EMT is a peculiar property of castration-resistant PCa cells, such as PC-3 and DU145, which express low levels of androgen receptor (AR), and 22Rv-1, which express high levels of AR but are androgen refractory (Supplementary Fig. S8). On the contrary, the androgen-sensitive LNCaP cells are unable to undergo CAF-mediated EMT, while remaining responsive to E-Cadherin upregulation promoted by the ectopic expression of *miR-205* (Supplementary Fig. S8).

Once ascertained the capability of *miR-205* to interfere with the afferent pathway [*i.e.*, CAF-promoted EMT in PCa cells (23)], we verified whether the miRNA also affects the efferent pathway, that is the tumor-induced activation of fibroblasts. Given that IL-6 is the main soluble factor produced by PCa cells to activate the surrounding stroma (23), cytokine amounts were measured in the CM of PC-3 cells exposed to different stimuli (Fig. 6A). Ectopic *miR-205* overexpression was found to counteract the enhancement of IL-6 secretion triggered by CAFs, as assessed by western immunoblotting (Fig. 6A, top) and enzyme-linked immunosorbent assay (ELISA) (Fig. 6A, bottom). As a consequence, media from *miR-205*-expressing PC-3 cells stimulated with CAFs were unable to promote activation of normal prostatic fibroblasts, as assessed by measuring fibroblast activation protein expression levels (Fig. 6B). Accordingly, such fibroblasts could not enhance PCa cell invasion (Fig. 6C).

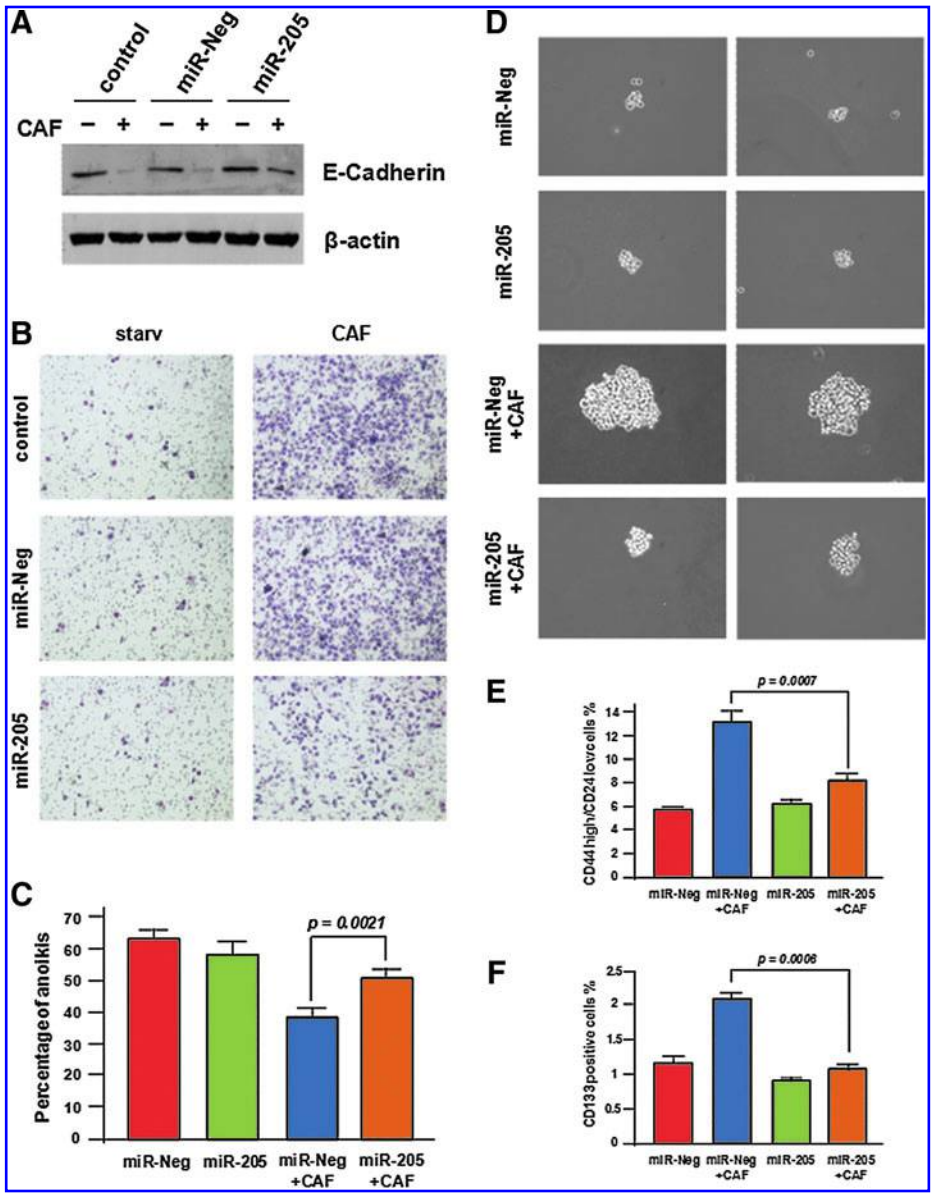

FIG. 5. ***miR-205*** **prevents CAF-induced EMT in PCa cells** ***in vitro*****. (A)** PC-3 cells were transfected at low cell density (1×10^5/p100) with *miR-205* precursor or with miR-Neg and, after 48 h, treated or not with the CM from CAFs for an additional 48 h. The levels of E-cadherin were assessed by immunoblotting. Vehicle-transfected cells were used as a control. **(B)** Invasion of PC-3 cells, treated as in **(A),** was analyzed (24 h of invasion toward complete growth medium). Photographs are representative of six randomly chosen fields. **(C)** PC-3 cells treated as in **(A)** were detached and maintained in suspension for 48 h. Anoikis was quantified by FACS analysis as the percentage of annexin V/propidium-iodide-positive cells. After detachment, PC-3 cells were also analyzed for their clonogenic potential. First-passage individual prostaspheres were photographed **(D)**, and the percentage of $CD44^{high}/CD24^{low}$ cells **(E)** and CD133-positive cells **(F)** was analyzed by FACS analysis (data are reported as mean ± standard deviation of four experiments). FACS, fluorescence activated cell sorter. To see this illustration in color, the reader is referred to the web version of this article at www.liebertpub.com/ars

By analyzing gene expression profiles obtained for DU145 PCa cells restored in *miR-205* expression (GSE11701 dataset) (19), enrichment of gene sets related to cytokine and chemokine activity (including IL-6) was observed among genes downmodulated by the miRNA (Fig. 6D and Supplementary Table S4), thus confirming the ability of *miR-205* to repress IL-6 production by PCa cells. On the same dataset, and consistent with the role of *miR-205* in counteracting the EMT program, inverse expression patterns were identified between *miR-205* and genes involved in metastasis or TGF-β signaling (Fig. 6D and Supplementary Table S4). Enrichment of gene sets related to the IL-6 pathway was also found among genes negatively correlated with *miR-205* expression in Taylor's set of clinical samples (highlighted in red in Supplementary Table S3). Modulation of IL-6 by *miR-205* may be the result of the simultaneous suppression of a number of oncogenes that we previously showed to be potentially targeted by the miRNA (19). Among these, protein kinase C epsilon (PKCε) has been specifically shown to enhance STAT3 localization onto the IL-6 promoter and thereby increase IL-6 expression (30). It is hence very likely that suppression of PKCε by *miR-205* may result in reduced transcription and secretion of IL-6. To further support this hypothesis we measured IL-6 expression levels in PC-3 cells silenced for PKCε and found that they were downmodulated, thus phenocopying *miR-205* effect (Fig. 6E).

Altogether, such findings suggest that *miR-205* downmodulation is a prerequisite for the completion of CAF-induced EMT in PCa cells and for the acquisition of activating properties toward surrounding fibroblasts.

To validate this finding *in vivo*, we analyzed the effects of *miR-205* modulation on tumor growth and lung colonization of PCa cells. As previously reported, prostate CAFs powerfully prompt tumor growth and metastatic spread to lungs (23). *miR-205* overexpressing PC-3 cells were s.c. coinoculated with CAFs in the lateral flanks of SCID bg/bg mice, under conditions (*i.e.*, 1×10^6/flank and in the absence of Matrigel) that prevent their *in vivo* growth in the absence of activated fibroblasts (5). As shown in Figure 7A, ectopic

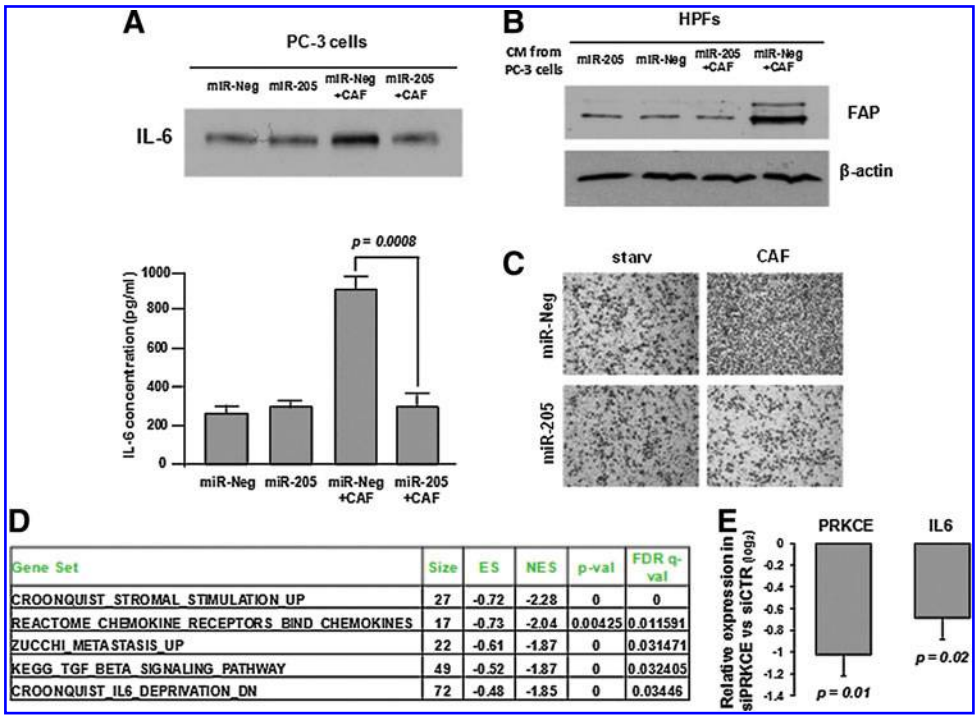

Gene Set	Size	ES	NES	p-val	FDR q-val
CROONQUIST_STROMAL_STIMULATION_UP	27	-0.72	-2.28	0	0
REACTOME_CHEMOKINE_RECEPTORS_BIND_CHEMOKINES	17	-0.73	-2.04	0.00425	0.011591
ZUCCHI_METASTASIS_UP	22	-0.61	-1.87	0	0.031471
KEGG_TGF_BETA_SIGNALING_PATHWAY	49	-0.52	-1.87	0	0.032405
CROONQUIST_IL6_DEPRIVATION_DN	72	-0.48	-1.85	0	0.03446

FIG. 6. ***miR-205* prevents CAF activation by PCa cells. (A)** PC-3 cells were transfected at low cell density (1×10^5/p100) with *miR-205* precursor or with pre-miR-Neg as a control and, after 48 h, treated or not with CM from CAFs for an additional 48 h. Secreted IL-6 was evaluated by immunoblotting (*top*) and quantified by enzyme-linked immunosorbent assay (IL-6 concentration was normalized on protein content) (*bottom*) in the CM of the above treated cells. **(B)** HPFs were incubated with CM from PC-3 cells (treated as in **A**) for 48 h. Fibroblast activation protein (FAP) expression was assessed by immunoblotting on cell lysates. **(C)** Invasion of PC-3 cells, treated with CMs derived from the differently treated HPFs **(**see **B)**, was analyzed (24 h of invasion toward complete growth medium). Photographs are representative of four randomly chosen fields. **(D)** Representative gene sets significantly enriched among genes downregulated after *miR-205* restoring in DU145 PCa cells (dataset GSE11701), including gene sets related to cytokine activity, are reported. **(E)** qRT-PCR assessment of PKCε (*PRKCE*) and *IL6* mRNA expression levels in PC-3 cells transfected with siRNA against PKCε (siPRKCE). Data are reported as $\log_2$-relative quantity compared to cells transfected with control siRNA (siCTR). IL-6, interleukin-6; PKCε, protein kinase C epsilon. To see this illustration in color, the reader is referred to the web version of this article at www.liebertpub.com/ars

miR-205 expression significantly impaired tumor growth of PC-3 cells co-injected with CAFs. In addition, an experimental metastasis assay in which PCa cells (22), modulated or not for *miR-205* expression, were first exposed *in vitro* to CAFs to induce EMT and then injected into the tail vein of SCID bg/bg mice showed that *miR-205* upregulation markedly inhibited the ability of PCa cells to colonize lungs (as detected by number of micrometastases in animals sacrificed after 8 weeks), highlighting the key role of the miRNA in PCa metastatic dissemination (Fig. 7B, C).

miR-205 reverts CAF-induced EMT

To assess the therapeutic potential of *miR-205* reconstitution approach, we investigated whether restoring expression of the miRNA was able to revert the mesenchymal phenotype of PCa cells that had already undergone CAF-induced EMT. Specifically, PC-3 cells were stimulated with the CM from in vitro-activated HPFs or CAFs for 48 h to induce EMT and subsequently transfected with *miR-205* precursor or, for comparative purposes, with siRNA against COX-2 or HIF-1α. The replacement of *miR-205* was found to successfully revert EMT induced by activated fibroblasts, as detected by changes in cell morphology (Fig. 8A) and increased E-cadherin expression (Fig. 8B), whereas silencing of HIF-1α or COX-2 (assessment of their knockdown is reported in Supplementary Fig. S9) did not (Fig. 8A, B). Such findings confirm the hierarchy between miRNA downregulation and activation of the COX-2/HIF-1α-dependent pro-inflammatory axis (Fig. 8C) and suggest that compounds targeting such a pathway may be ineffective to treat cancer cells that have already undergone EMT once they have experienced miRNA downregulation.

Discussion

The impact of miRNAs on tumor microenvironment has been addressed thus far by only few studies. The first evidence of their involvement in the dynamic crosstalk between the tumor and the surrounding stroma was provided by Aprelikova *et al.* (1), who identified *miR-31* as the most downregulated miRNA in CAFs isolated from endometrial cancers compared with fibroblasts derived from normal adjacent tissues. Functionally, CM from CAFs ectopically overexpressing *miR-31* reduced migration and invasion of EC1 endometrial cancer cells, suggesting that *miR-31* may target genes responsible for the secretion of soluble factors implicated in promoting tumor cell sprouting (1). Concerning PCa, the only available information indicates that *miR-15* and *miR-16* downregulation in CAFs promotes tumor growth and progression through reduced post-transcriptional repression

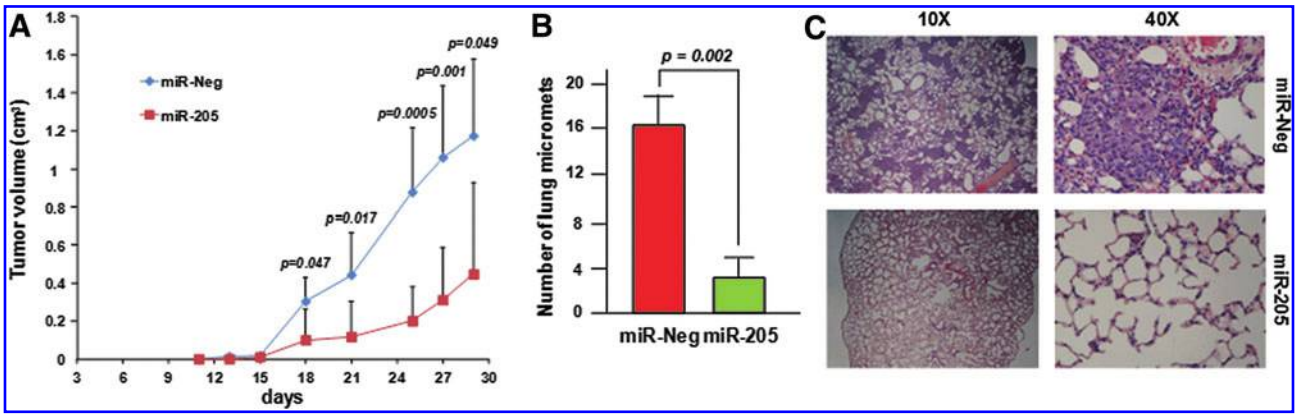

FIG. 7. ***miR-205*** **prevents CAF-induced enhancement of PCa cell tumorigenicity and metastatic dissemination** ***in vivo*****.** **(A)** PC-3 xenograft growth in SCID bg/bg mice. A mixture of 1×10^6 PC-3 cells transfected either with *miR-205* precursor or miR-Neg and 0.5×10^6 CAFs was subcutaneously injected ($n=8$ mice per group). The onset and volume of the primary tumor are reported in the growth curve. *P*-values of the difference between tumor volumes in the two groups at each time point (*miR-205 vs.* miR-Neg) are reported. **(B)** PC-3 lung colonization in SCID bg/bg mice. PC-3 cells were transfected either with *miR-205* precursor or miR-Neg and after 48 h were treated with CM from CAFs. After 72 h, cells were injected into the lateral tail vein of mice ($n=8$ per group). Animals were monitored at 3-day intervals and were sacrificed after 8 weeks. Lungs were inspected with the aid of a microscope and micrometastases were counted. **(C)** Paraffin-embedded tissue sections from lung micrometastases (original magnification 10× and 40×) obtained by *miR-205*- or miR-Neg-transfected PC-3 cells injected in SCID bg/bg mice were stained with hematoxylin and eosin.

of fibroblast growth factor-2 and its receptor FGFR1, which act on both stromal and tumor cells to enhance cancer cell survival, proliferation, and migration (41). However, no evidence is currently available on miRNAs that either regulate pathways activated in tumor cells upon CAF contact or influence the capability of tumor cells to activate surrounding stroma. The identification of such miRNAs might set the rationale for developing specific therapeutic approaches.

In the present study, we explored the modulation of miRNA expression in PCa cells upon stimulation with patient-derived CAFs. Consistent with induction of an EMT phenotype, miRNAs known to be associated with the process, such as *miR-200* family members, were markedly downmodulated. However, changes in the expression of other miRNAs with unknown function or at least with undocumented participation in EMT were observed, suggesting that we are still far from understanding which pathways are activated in cancer cells upon interaction with their microenvironment. The most downmodulated miRNA was *miR-205*. We previously reported that *miR-205* exerts a tumor-suppressive effect in PCa cells by inducing a mesenchymal-epithelial transition (MET) and the concomitant downregulation of oncogenes involved in disease progression (*i.e.*, IL-6, PKCε, caveolin-1, and EZH2) (19).

Consistent with such tumor-suppressive function, *miR-205* expression levels appear reduced in tumors, especially those from patients with disease spread to regional lymph nodes, suggesting a functional role of *miR-205* loss in PCa dissemination (19,20,57). In keeping with these findings, here we show that *miR-205* expression is almost completely lost in PCa metastases, which emerged from the analysis of a large publicly available dataset. In addition, reduced *miR-205* levels in primary tumors correlated with increased risk for patients experiencing biochemical recurrence after radical prostatectomy. Recently, we also showed that *miR-205* can enhance basement membrane deposition both by normal and tumor cells, thus conferring to the miRNA a further repressive function against metastatic dissemination (21).

Marked downregulation of *miR-205* in cells undergoing EMT upon CAF stimulation is consistent with the aforementioned roles played by the master regulator miRNA. Noteworthy is the observation that *miR-205* can be responsive to stromal signals, in addition to the reported regulation by TGF-β in Madin–Darby canine kidney cells (25). The participation of *miR-205* in EMT induced by stimuli other than TGF-β is not trivial, considering that signals relevant for the metastatic spur induced by stroma interactions have not yet been identified. Notably, only androgen-refractory PCa cells undergo EMT in response to CAFs, and they do it in a *miR-205*-dependent manner. This finding would suggest that the malignant interplay between cancer and stromal cells is mainly effective in aggressive and hormonal therapy-resistant PCas.

MiR-205 downmodulation in clinical PCa may hence be the result of crosstalk between epithelial cells and fibroblasts. Obviously, it is hard to say whether mutations in epithelial cells converting them into tumor cells precede activation of fibroblasts, or whether epigenetic changes within the microenvironment can *per se* transform epithelial cells. An established finding is that activated stroma can exacerbate *miR-205* downmodulation in cancer cells, thus prompting EMT and metastasis. In this regard, stimulation of PCa cells by CAFs needs to be continuous to maintain EMT features. It is possible that PCa cells may leave the primary tumor together with associated fibroblasts to maintain their mesenchymal traits, consistent to what was observed for Lewis lung carcinoma cell model (15), where stromal cells from the primary tumor site were detected in metastatic nodules spontaneously formed in mouse lungs after resection of subcutaneously grown xenografts. The data highlight how metastatic cancer cells may bring their own soil, including activated fibroblasts, from the primary site to the colonized organs.

In the present study, HIF-1α has been acknowledged as a direct transcriptional repressor of *miR-205*, corroborating previous data showing miRNA downmodulation in human placental trophoblasts under hypoxic conditions (39). The

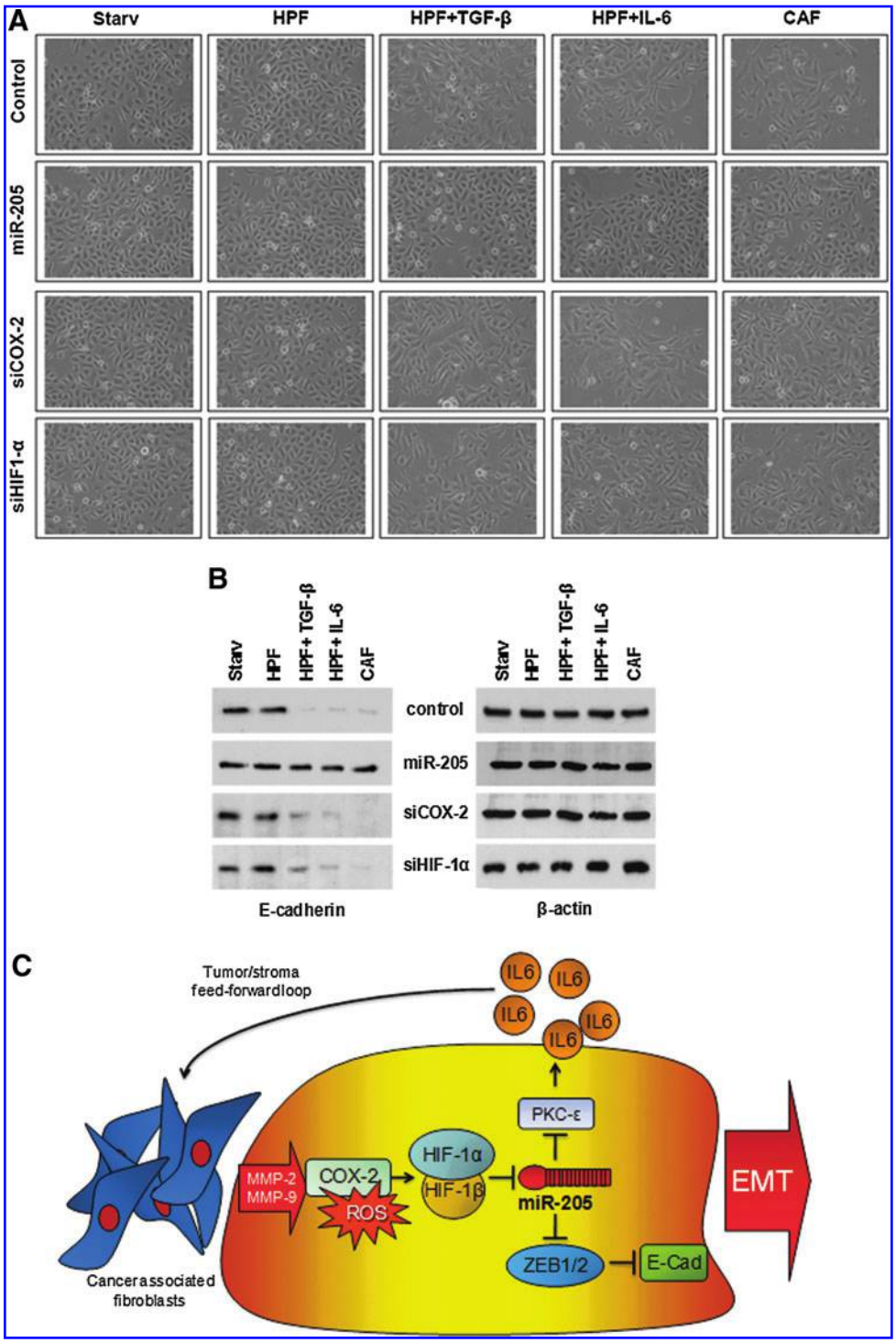

FIG. 8. *miR-205* reverts CAF-induced EMT. PC-3 cells were treated with the CM from *in vitro* activated HPFs (10 ng/ml TGF-β1 or 50 ng/ml IL-6) or from CAFs for 48 h to induce EMT and then transfected with *miR-205* precursor or silenced with siRNAs against COX-2 or HIF-1α. After 48 h, cell morphology **(A)** and the levels of E-cadherin **(B)** were assessed. Photographs are representative of randomly chosen fields. **(C)** Schematic representation of the central role played by *miR-205* in the crosstalk between CAFs and PCa cells. CAFs secrete MMP-2 and MMP-9, which activate EMT and stemness in PCa cells, by promoting the COX-2 pro-inflammatory pathway. ROS produced by COX-2 activity favor a redox-dependent stabilization of HIF-1 (18,22), which, in turn, induces *miR-205* transcriptional repression. Downregulation of the miRNA leads to derepression of its targets ZEB1/2 and PKC-ε (19), thus allowing respectively EMT and IL-6 secretion by PCa cells. By these two pathways *miR-205* controls motility and stemness of PCa cells on one hand, and CAFs reactivity on the other, thereby closing the feed-forward loop between cancer and stromal cells. TGF-β1, tumor growth factor-β1; MMP, matrix metalloprotease; ROS, reactive oxygen species. To see this illustration in color, the reader is referred to the web version of this article at www.liebertpub.com/ars

capability of HIF-1α to function as a transcriptional repressor, besides being a well-known transcriptional activator, has been recently demonstrated in different cell models (9,16,17,38,58). Several mechanisms have been proposed to mediate the transcriptional repression activity of HIF-1α. Specifically, in addition to a direct transcriptional repressor activity (9,43), indirect mechanisms involving the recruitment of already acknowledged HIF-induced transcriptional co-repressors (17,33) have been suggested. Although at present we do not have a comprehensive knowledge of the molecular events engaged by CAFs to convert HIF-1α into a transcriptional repressor, we obtained several lines of evidence suggesting HIF-1α repressive role on *miR-205* transcription. First, silencing of HIF-1α severely prevented *miR-205* downregulation induced by CAF treatment. Second, ChIP analysis confirmed an increase in *miR-205* promoter occupancy by HIF-1α upon CAF stimulation, by binding to three HIF-1-responsive elements. Third, the modulation of HIF-1α levels by culturing PC-3 cells under hypoxic conditions or in the presence of $CoCl_2$ induced a clear downregulation of *miR-205*

primary transcript, thus confirming that HIF-1α can ultimately repress the transcription of the miRNA.

The key upstream regulator of HIF-1α is confirmed as COX-2, which we already acknowledged as a source of oxidants essential to stabilize the HIF-1α subunit and allow EMT of PCa cells (22). HIF-1α can also be viewed as a mandatory crossroad that drives cancer cells toward malignancy (6,10,13,35,54) in which *miR-205* and oxidative stress play a pleiotropic role. The role of oxidative stress, a common feature of aggressive cancers, in regulating miRNAs that control EMT is still unclear. Indeed, although oxidative stress has been widely reported as positively correlated with EMT activation, expression of *miR-200a* leads to an increase in oxidative stress in ovarian tumors (36).

Interestingly, activation of COX-2 and HIF-1α is just a transient phenomenon during CAF-induced EMT. For this reason, targeting such factors may be not promising for therapeutic purposes. We actually observed that once PCa cells have experienced EMT, silencing of either COX-2 or HIF-1α is ineffective. In contrast, ectopic overexpression of *miR-205*, which represents the final mediator of CAF-induced EMT by directly repressing ZEB1/2 (19,25), can both prevent and revert the acquisition of mesenchymal features induced by stromal signals. The effects of *miR-205* overexpression spread to several key features of metastatic cells, including the ability to cross the ECM barrier and invade tissues, the resistance to *anoikis* allowing survival in the bloodstream, and the achievement of stem-like traits. To the best of our knowledge, *miR-205* is the first example of a miRNA that, once exogenously modulated in tumor cells, can impede activation of and by surrounding fibroblasts. In keeping with this, forced expression of *miR-205* leads to interruption of the "efferent" pathway engaged by cancer cells and leading to stromal reactivity. Such evidence further justifies the opportunity to utilize *miR-205* as a tool to prevent or counteract PCa metastasis. *In vivo* data generated in the present study support the capability of *miR-205* to reduce tumor growth, presumably by inhibiting local invasion, and lung colonization. The latter effect may depend on either increased *anoikis* of *miR-205*-expressing PCa cells, which therefore would not survive in circulation, or reduced extravasation (or both), thus ultimately leading to impaired metastasis formation. The results also highlight the relevance of MET during tumor dissemination. EMT in tumor cells needs indeed to be transient. During early steps of metastasis, tumor cells undergo EMT in response to external cues at the invasive front to gain a more motile and invasive mesenchymal phenotype. However, once a metastatic cell has invaded a new tissue, it needs to revert to a more epithelial phenotype to efficiently settle down and grow as a metastasis. The need to maintain a certain degree of plasticity justifies the reversibility of CAF-induced EMT, as observed in the present study. From our standpoint, MET has to occur after cells exit from the bloodstream, likely due to stromal signals from the host secondary organ. Cells undergoing MET when still in the circulation, such as *miR-205*-expressing cells in our metastasis assay, are actually unable to metastasize. This is in contrast with data of Korpal *et al.* (32) showing that *miR-200*s replacement in 4TO7 mouse mammary tumor cells can even favor colonization when cells are intravenously injected. Presumably, the roles of *miR-205* and *miR-200*s in EMT/MET are not completely overlapping.

Overall, the evidence collected so far will be instrumental to properly shape *miR-205*-based therapeutic approaches. Overexpression of miRNA in the primary tumor by local delivery could be specifically envisaged to prevent local invasion and intravasation, thus blocking initial dissemination. However, effective anti-metastatic therapy should impair the survival and colonization capabilities of already disseminated tumor cells and not simply prevent detachment from the primary tumor. Notably, circulating tumor cells can be detected in patients with very early neoplastic lesions (42). For this purpose, systemic therapeutic approaches should be preferable. Obviously, this can be accomplished only when systems to selectively deliver therapeutic miRNAs to the cells of interest become available, thus avoiding their overexpression in unwanted tissues and limiting potential side effects.

Materials and Methods

See Supplementary Data for a detailed description of miRNA expression profiling, miRNA and gene expression analysis, ChIP, western blot analysis, and Boyden invasion assay.

Experimental models

Human PCa cells (PC-3, DU145, LNCaP, and 22Rv-1) were obtained from the European Collection of Cell Cultures and maintained at 37°C/5% carbon dioxide in Dulbecco's modified Eagle's medium (DMEM) supplemented with 10% fetal bovine serum. For hypoxia experiments, PC-3 cells were maintained at a constant gas mixture of 1% oxygen, 94% nitrogen, and 5% carbon dioxide in a specially designed hypoxia incubator (Galaxy® 48 R Eppendorf). Control cells were maintained in 20% oxygen. $CoCl_2$ was administered at the final concentration of 150 μM.

Human prostate fibroblasts (HPFs and CAFs) were isolated from surgical explantation after patient informed consent in accord with the Ethics Committee of the *Azienda Ospedaliera Universitaria Careggi*. Briefly, HPFs and CAFs were extracted from healthy and intratumoral regions of the prostate of PCa-bearing patients (average Gleason = 4 + 4, all pT3aN0). Tissue samples were aseptically obtained from patients undergoing radical prostatectomy. Tissues were digested overnight in 1 mg/ml collagenase I, and cells were plated in DMEM containing 10% fetal bovine serum. CM from HPFs and CAFs was obtained by 48-h serum-starved cells, clarified by centrifugation, and used freshly.

Fibroblast activation

HPFs were grown to subconfluence and treated for 24 h with 10 ng/ml rTGF-β1, 50 ng/ml IL-6, or CM from PC-3 cells. Fresh serum-free medium was added for an additional 24 h before collection of CM.

Transfection

miR-205 precursor and negative control (miR-Neg) were purchased as Pre-miR™ miRNA precursor molecules (Life Technologies, Carlsbad, CA). miRCURY LNA Inhibitor specific for *miR-205* (LNA-205) and the negative control (LNA-Neg) were purchased from EXIQON (Woburn, MA). Cells seeded at the appropriate density were transfected for 4 h at 37°C with 20 n*M* miRNA precursors or 100 n*M* miRNA

inhibitors using Lipofectamine-2000 (Life Technologies), according to the manufacturer's instruction, and processed at different time intervals.

For silencing experiments, siCOX-2 (sc-29279; Santa Cruz Biotechnology, Santa Cruz, CA), siHIF1-α (5'-AAAGGA CAAGUCACCACAGGA-3'; Qiagen, Hilden, Germany), control siRNA (16), or siPRKCE (19) were administered at a final concentration of 20 n*M*, using Lipofectamine-2000.

miRNA expression profiling

Total RNA was isolated from PC-3 cells using TRIzol (Life Technologies) reagent, then miRNAs were profiled on the Illumina Human v2 MiRNA expression beadchip (Illumina, San Diego, CA), according to the manufacturer's instructions. All array data have been deposited in National Center for Biotechnology Information's Gene Expression Omnibus (GEO, www.ncbi.nlm.nih.gov/geo/), according to MIAME (minimum information about a microarray experiment) guidelines, and assigned the identifier GSE42699. Hierarchical clustering and class comparison to identify differentially expressed miRNAs were carried out using BRB-ArrayTools Version: 4.2.0- B_2 (June 2011), developed by Drs. Richard Simon and Amy Peng Lam (http://linus.nci.nih.gov/BRB-ArrayTools.html). See Supplementary Data for further details.

Analysis of publicly available datasets

Processed gene and miRNA expression data used in Taylor *et al.* (52) were downloaded from GEO (GSE21032). *miR-205* expression levels in normal prostate tissue, primary prostate carcinoma, and metastatic lesions were extracted. Primary tumors from patients who underwent chemo-, radio-, or androgen ablation therapy prior to prostatectomy were excluded from the analysis. The Cox model and Kaplan–Meier method were used to test the association between *miR-205* expression and biochemical relapse. Expression values were dichotomized defining as "miR-low" 17% of primary tumors with the lowest expression levels.

Using the 98 samples (normal prostate tissue, primary prostate carcinoma, metastatic lesions, and cell lines) with available gene and miRNA data, *miR-205* expression levels were correlated with expression levels of all 19,839 genes (Spearman correlation). Hence, genes were ordered according to their correlation with *miR-205*, and a GSEA was performed (GSEA 2.0, Preranked analysis), testing the "C2" gene sets collection of the Molecular Signatures Database v3.0 (www.broadinstitute.org/gsea). The same gene sets were tested (GSEA 2.0) on the GSE11701 dataset containing expression data of DU145 PCa cells restored or not for *miR-205* expression. Gene sets with false discovery rate < 5% were considered statistically enriched.

miRNA and gene expression analysis

miR-205, *miR-200b*, pri-*miR-205*, E-cadherin, Drosha, Dicer, *ZEB1*, *ZEB2*, *SNAI1*, *SNAI2*, *TWIST1*, *PRKCE*, and *IL6* mRNA expression was assessed by qRT-PCR as detailed in Supplementary Data.

Chromatin immunoprecipitation

The presence and position of putative HIF-1α binding sites within the *miR-205* promoter region was predicted using the Jaspar algorithm (http://jaspar.genereg.net/), setting a cutoff ≥ 0.85. ChIP experiments were carried out as described in Orlotti *et al.* (45). Briefly, chromatin from PC-3 cells was immunoprecipitated overnight at 4°C using 4 μg of mouse monoclonal antibody to HIF-1α (Abcam, Cambridge, UK) or normal mouse preimmuned IgG (Upstate Biotechnology, Lake Placid, NY) as a negative control. DNA from immunoprecipitants was then analyzed by PCR using primers flanking the HIF-1α putative binding sites. For PCR analysis, aliquots of chromatin before immunoprecipitation were saved (Input). See Supplementary Data for further details.

Prostasphere formation and clonogenicity assay

PC-3 cells, modulated for *miR-205* expression, were incubated for 72 h with CM from CAFs and then detached using Accutase (Sigma-Aldrich, St. Louis, MO). For prostasphere formation, single cells were plated at 150 cells/cm^2 on low-attachment 100-mm plates (Corning Inc., Corning, NY) in DMEM/F12 (Life Technologies) supplemented with B27 and N2 (Life Technologies), 5 μg/ml insulin, 20 ng/ml basic fibroblast growth factor, and 20 ng/ml epidermal growth factor. Cells were grown under these conditions for 15–20 days and formed non-adherent P0 spheres termed prostaspheres. For the evaluation of self-renewal, a single prostasphere was dissociated in single cells with Accutase, and a dilution of one cell per well into 96-well low-attachment plates was performed to isolate individual P1 prostaspheres.

Flow cytometry

PC-3 cells (1×10^6), modulated for *miR-205* expression, were incubated for 72 h with CM from CAFs and then were labeled with FITC-anti-CD44 (clone G44-26) and PE-anti-CD24 (clone ML5) antibodies for 1 h at 4°C in the dark. Cells were washed, and flow cytometry was performed using a FACScan (BD Biosciences, Franklin Lakes, NJ).

IL-6 quantification by ELISA

Determination of IL-6 concentration in cell culture media was performed by Chemiluminescence ELISA Kit according to the manufacturer's instructions (Life Technologies, Cat. No. KHC0069). The IL-6 ELISA was linear between 5 and 4000 pg/ml. Cell culture supernatant samples were diluted fourfold in Standard Diluent Buffer and 100 μl of the diluted samples were used to run the assay.

Xenograft experiments

In vivo experiments were carried out in accord with national guidelines and approved by the Ethics Committee of the Animal Welfare Office of the Italian Work Ministry and conformed to the legal mandates and Italian guidelines for the care and maintenance of laboratory animals. Male SCID-bg/bg mice (6–8 weeks old; Charles River Laboratories International Inc., Wilmington, MA) were injected subcutaneously, both in the right and left lateral flanks, with 1×10^6 PC-3 cells (modulated in *miR-205* expression) plus 0.5×10^6 CAFs, in a total volume of 0.1 ml phosphate-buffered saline. Animals (eight per group) were monitored daily, and tumor size was measured every 2–3 days by a caliper. Tumor volumes were determined by the length (L) and the width (W): $V = (LW^2)/2$. Mice were sacrificed before the tumor masses exceeded a size to produce evident

physical discomfort, such as a rough looking hair coat, lack of grooming activity, or abnormal posture (huddling, hunching, or being stiff). Excised tumors were fixed overnight at 4°C in formalin (5% in phosphate buffered saline) for histologic analyses. Formalin-fixed, paraffin-embedded tissue blocks were cut into 5 μm consecutive sections and mounted on positively charged slides. Tissue sections were deparaffinazed and rehydrated before staining with hematoxylin and eosin.

Lung colonization assays

Male SCID-bg/bg mice (6–8 weeks old) were injected with PC-3 previously transfected with *miR-205* precursor or miR-Neg and, after 48 h, treated *ex vivo* with CM from CAFs for an additional 72 h. Mice (eight animals per group) were injected in the lateral tail veins with the differently treated PC-3 cells (1×10^6 in 0.1 ml of phosphate-buffered saline). Animals were monitored every 3 days and sacrificed after 8 weeks. Lungs were inspected for micrometastases by histological analyses.

Statistical analysis

Data are presented as mean values ± standard deviation from at least three independent experiments. Statistical analysis of the data was performed by two-tailed Student's *t* test. *P*-values < 0.05 were considered statistically significant. Statistics applied to microarray analyses is described in the relative sections.

Acknowledgments

We thank Dr. Valentina Profumo for useful suggestions; Dr. Valentina Doldi and Dr. Luigi Carlessi for technical advice and institutional Functional Genomics Core Facility for microarray analysis. We also thank Mrs. Betty Johnston for editing the article.

The work in the authors' laboratory is supported by the Italian Association for Cancer Research (AIRC), Special Program "Innovative Tools for Cancer Risk Assessment and Early Diagnosis," 5 × 1000, (project No. 12162), (N.Z., R.V., M.A.P.); AIRC grants (No. 11542, 8797), (P.G., P.C.); Istituto Toscano Tumori (No. 0203607), (P.C.); and MIUR-PRIN 2008, (P.C.).

Author Disclosure Statement

No competing financial interests exist.

References

1. Aprelikova O, Yu X, Palla J, Wei BR, John S, Yi M, Stephens R, Simpson RM, Risinger JI, Jazaeri A, and Niederhuber J. The role of miR-31 and its target gene SATB2 in cancer-associated fibroblasts. *Cell Cycle* 9: 4387–4398, 2010.
2. Bartel DP. MicroRNAs: target recognition and regulatory functions. *Cell* 136: 215–233, 2009.
3. Bhatnagar N, Li X, Padi SK, Zhang Q, Tang MS, and Guo B. Downregulation of miR-205 and miR-31 confers resistance to chemotherapy-induced apoptosis in prostate cancer cells. *Cell Death Dis* 1: e105, 2010.
4. Bhowmick NA, Chytil A, Plieth D, Gorska AE, Dumont N, Shappell S, Washington MK, Neilson EG, and Moses HL. TGF-beta signaling in fibroblasts modulates the oncogenic potential of adjacent epithelia. *Science* 303: 848–851, 2004.
5. Bhowmick NA, Neilson EG, and Moses HL. Stromal fibroblasts in cancer initiation and progression. *Nature* 432: 332–337, 2004.
6. Calvani M, Comito G, Giannoni E, and Chiarugi P. Time-dependent stabilization of hypoxia inducible factor-1alpha by different intracellular sources of reactive oxygen species. *PLoS One* 7: e38388, 2012.
7. Cannito S, Novo E, di Bonzo LV, Busletta C, Colombatto S, and Parola M. Epithelial-mesenchymal transition: from molecular mechanisms, redox regulation to implications in human health and disease. *Antioxid Redox Signal* 12: 1383–1430, 2010.
8. Castellon EA, Valenzuela R, Lillo J, Castillo V, Contreras HR, Gallegos I, Mercado A, and Huidobro C. Molecular signature of cancer stem cells isolated from prostate carcinoma and expression of stem markers in different Gleason grades and metastasis. *Biol Res* 45: 297–305, 2012.
9. Chen KF, Lai YY, Sun HS, and Tsai SJ. Transcriptional repression of human cad gene by hypoxia inducible factor-1alpha. *Nucleic Acids Res* 33: 5190–5198, 2005.
10. Chiavarina B, Whitaker-Menezes D, Migneco G, Martinez-Outschoorn UE, Pavlides S, Howell A, Tanowitz HB, Casimiro MC, Wang C, Pestell RG, Grieshaber P, Caro J, Sotgia F, and Lisanti MP. HIF1-alpha functions as a tumor promoter in cancer associated fibroblasts, and as a tumor suppressor in breast cancer cells: autophagy drives compartment-specific oncogenesis. *Cell Cycle* 9: 3534–3551, 2010.
11. Cirri P, and Chiarugi P. Cancer associated fibroblasts: the dark side of the coin. *Am J Cancer Res* 1: 482–497, 2011.
12. Cirri P, and Chiarugi P. Cancer-associated-fibroblasts and tumour cells: a diabolic liaison driving cancer progression. *Cancer Metastasis Rev* 31: 195–208, 2012.
13. Comito G, Giannoni E, Di GP, Segura CP, Gerlini G, and Chiarugi P. Stromal fibroblasts synergize with hypoxic oxidative stress to enhance melanoma aggressiveness. *Cancer Lett* 324: 31–41, 2012.
14. De WO, and Mareel M. Role of tissue stroma in cancer cell invasion. *J Pathol* 200: 429–447, 2003.
15. Duda DG, Duyverman AM, Kohno M, Snuderl M, Steller EJ, Fukumura D, and Jain RK. Malignant cells facilitate lung metastasis by bringing their own soil. *Proc Natl Acad Sci U S A* 107: 21677–21682, 2010.
16. Eltzschig HK, Abdulla P, Hoffman E, Hamilton KE, Daniels D, Schonfeld C, Loffler M, Reyes G, Duszenko M, Karhausen J, Robinson A, Westerman KA, Coe IR, and Colgan SP. HIF-1-dependent repression of equilibrative nucleoside transporter (ENT) in hypoxia. *J Exp Med* 202: 1493–1505, 2005.
17. Feige E, Yokoyama S, Levy C, Khaled M, Igras V, Lin RJ, Lee S, Widlund HR, Granter SR, Kung AL, and Fisher DE. Hypoxia-induced transcriptional repression of the melanoma-associated oncogene MITF. *Proc Natl Acad Sci U S A* 108: E924–E933, 2011.
18. Fiaschi T, Giannoni E, Taddei ML, Cirri P, Marini A, Pintus G, Nativi C, Richichi B, Scozzafava A, Carta F, Torre E, Supuran CT, and Chiarugi P. Carbonic anhydrase IX from cancer-associated fibroblasts drives epithelial-mesenchymal transition in prostate carcinoma cells. *Cell Cycle* 12: 1791–1801, 2013.
19. Gandellini P, Folini M, Longoni N, Pennati M, Binda M, Colecchia M, Salvioni R, Supino R, Moretti R, Limonta P, Valdagni R, Daidone MG, and Zaffaroni N. miR-205 Exerts tumor-suppressive functions in human prostate through down-regulation of protein kinase Cepsilon. *Cancer Res* 69: 2287–2295, 2009.

20. Gandellini P, Folini M, and Zaffaroni N. Towards the definition of prostate cancer-related microRNAs: where are we now? *Trends Mol Med* 15: 381–390, 2009.
21. Gandellini P, Profumo V, Casamichele A, Fenderico N, Borrelli S, Petrovich G, Santilli G, Callari M, Colecchia M, Pozzi S, De CM, Folini M, Valdagni R, Mantovani R, and Zaffaroni N. miR-205 regulates basement membrane deposition in human prostate: implications for cancer development. *Cell Death Differ* 19: 1750–1760, 2012.
22. Giannoni E, Bianchini F, Calorini L, and Chiarugi P. Cancer associated fibroblasts exploit reactive oxygen species through a proinflammatory signature leading to epithelial mesenchymal transition and stemness. *Antioxid Redox Signal* 14: 2361–2371, 2011.
23. Giannoni E, Bianchini F, Masieri L, Serni S, Torre E, Calorini L, and Chiarugi P. Reciprocal activation of prostate cancer cells and cancer-associated fibroblasts stimulates epithelial-mesenchymal transition and cancer stemness. *Cancer Res* 70: 6945–6956, 2010.
24. Giannoni E, Parri M, and Chiarugi P. EMT and oxidative stress: a bidirectional interplay affecting tumor malignancy. *Antioxid Redox Signal* 16: 1248–1263, 2012.
25. Gregory PA, Bert AG, Paterson EL, Barry SC, Tsykin A, Farshid G, Vadas MA, Khew-Goodall Y, and Goodall GJ. The miR-200 family and miR-205 regulate epithelial to mesenchymal transition by targeting ZEB1 and SIP1. *Nat Cell Biol* 10: 593–601, 2008.
26. Hanahan D, and Weinberg RA. Hallmarks of cancer: the next generation. *Cell* 144: 646–674, 2011.
27. Hinz B, Phan SH, Thannickal VJ, Prunotto M, Desmouliere A, Varga J, De WO, Mareel M, and Gabbiani G. Recent developments in myofibroblast biology: paradigms for connective tissue remodeling. *Am J Pathol* 180: 1340–1355, 2012.
28. Hung CS, Liu HH, Liu JJ, Yeh CT, Chang TC, Wu CH, Ho YS, Wei PL, and Chang YJ. MicroRNA-200a and −200b mediated hepatocellular carcinoma cell migration through the epithelial to mesenchymal transition markers. *Ann Surg Oncol* 2012.
29. Kalluri R, and Zeisberg M. Fibroblasts in cancer. *Nat Rev Cancer* 6: 392–401, 2006.
30. Kang JW, Park YS, Lee DH, Kim JH, Kim MS, Bak Y, Hong J, and Yoon DY. Intracellular interaction of interleukin (IL)-32alpha with protein kinase Cepsilon (PKCepsilon) and STAT3 protein augments IL-6 production in THP-1 promonocytic cells. *J Biol Chem* 287: 35556–35564, 2012.
31. Klarmann GJ, Hurt EM, Mathews LA, Zhang X, Duhagon MA, Mistree T, Thomas SB, and Farrar WL. Invasive prostate cancer cells are tumor initiating cells that have a stem cell-like genomic signature. *Clin Exp Metastasis* 26: 433–446, 2009.
32. Korpal M, Ell BJ, Buffa FM, Ibrahim T, Blanco MA, Celia-Terrassa T, Mercatali L, Khan Z, Goodarzi H, Hua Y, Wei Y, Hu G, Garcia BA, Ragoussis J, Amadori D, Harris AL, and Kang Y. Direct targeting of Sec23a by miR-200s influences cancer cell secretome and promotes metastatic colonization. *Nat Med* 17: 1101–1108, 2011.
33. Manalo DJ, Rowan A, Lavoie T, Natarajan L, Kelly BD, Ye SQ, Garcia JG, and Semenza GL. Transcriptional regulation of vascular endothelial cell responses to hypoxia by HIF-1. *Blood* 105: 659–669, 2005.
34. Mani SA, Guo W, Liao MJ, Eaton EN, Ayyanan A, Zhou AY, Brooks M, Reinhard F, Zhang CC, Shipitsin M, Campbell LL, Polyak K, Brisken C, Yang J, and Weinberg RA. The epithelial-mesenchymal transition generates cells with properties of stem cells. *Cell* 133: 704–715, 2008.
35. Martinez-Outschoorn UE, Trimmer C, Lin Z, Whitaker-Menezes D, Chiavarina B, Zhou J, Wang C, Pavlides S, Martinez-Cantarin MP, Capozza F, Witkiewicz AK, Flomenberg N, Howell A, Pestell RG, Caro J, Lisanti MP, and Sotgia F. Autophagy in cancer associated fibroblasts promotes tumor cell survival: role of hypoxia, HIF1 induction and NFkappaB activation in the tumor stromal microenvironment. *Cell Cycle* 9: 3515–3533, 2010.
36. Mateescu B, Batista L, Cardon M, Gruosso T, de FY, Mariani O, Nicolas A, Meyniel JP, Cottu P, Sastre-Garau X, and Mechta-Grigoriou F. miR-141 and miR-200a act on ovarian tumorigenesis by controlling oxidative stress response. *Nat Med* 17: 1627–1635, 2011.
37. Mizuguchi Y, Specht S, Lunz JG, III, Isse K, Corbitt N, Takizawa T, and Demetris AJ. Cooperation of p300 and PCAF in the control of microRNA 200c/141 transcription and epithelial characteristics. *PLoS One* 7: e32449, 2012.
38. Morote-Garcia JC, Rosenberger P, Nivillac NM, Coe IR, and Eltzschig HK. Hypoxia-inducible factor-dependent repression of equilibrative nucleoside transporter 2 attenuates mucosal inflammation during intestinal hypoxia. *Gastroenterology* 136: 607–618, 2009.
39. Mouillet JF, Chu T, Nelson DM, Mishima T, and Sadovsky Y. MiR-205 silences MED1 in hypoxic primary human trophoblasts. *FASEB J* 24: 2030–2039, 2010.
40. Murphy MP. Modulating mitochondrial intracellular location as a redox signal. *Sci Signal* 5: e39, 2012.
41. Musumeci M, Coppola V, Addario A, Patrizii M, Maugeri-Sacca M, Memeo L, Colarossi C, Francescangeli F, Biffoni M, Collura D, Giacobbe A, D'Urso L, Falchi M, Venneri MA, Muto G, De MR, and Bonci D. Control of tumor and microenvironment cross-talk by miR-15a and miR-16 in prostate cancer. *Oncogene* 30: 4231–4242, 2011.
42. Nagrath S, Sequist LV, Maheswaran S, Bell DW, Irimia D, Ulkus L, Smith MR, Kwak EL, Digumarthy S, Muzikansky A, Ryan P, Balis UJ, Tompkins RG, Haber DA, and Toner M. Isolation of rare circulating tumour cells in cancer patients by microchip technology. *Nature* 450: 1235–1239, 2007.
43. Narravula S, and Colgan SP. Hypoxia-inducible factor 1-mediated inhibition of peroxisome proliferator-activated receptor alpha expression during hypoxia. *J Immunol* 166: 7543–7548, 2001.
44. Nieto MA, and Cano A. The epithelial-mesenchymal transition under control: global programs to regulate epithelial plasticity. *Semin Cancer Biol* 22: 361–368, 2012.
45. Orlotti NI, Cimino-Reale G, Borghini E, Pennati M, Sissi C, Perrone F, Palumbo M, Daidone MG, Folini M, and Zaffaroni N. Autophagy acts as a safeguard mechanism against G-quadruplex ligand-mediated DNA damage. *Autophagy* 8: 1185–1196, 2012.
46. Parri M, and Chiarugi P. Redox molecular machines involved in tumor progression. *Antioxid Redox Signal* 19: 1828–1845, 2013.
47. Pavlides S, Tsirigos A, Vera I, Flomenberg N, Frank PG, Casimiro MC, Wang C, Fortina P, Addya S, Pestell RG, Martinez-Outschoorn UE, Sotgia F, and Lisanti MP. Loss of stromal caveolin-1 leads to oxidative stress, mimics hypoxia and drives inflammation in the tumor microenvironment, conferring the "reverse Warburg effect": a transcriptional informatics analysis with validation. *Cell Cycle* 9: 2201–2219, 2010.
48. Pellacani D, Oldridge EE, Collins AT, and Maitland NJ. Prominin-1 (CD133) expression in the prostate and prostate cancer: a marker for quiescent stem cells. *Adv Exp Med Biol* 777: 167–184, 2013.

49. Piovan C, Palmieri D, Di LG, Braccioli L, Casalini P, Nuovo G, Tortoreto M, Sasso M, Plantamura I, Triulzi T, Taccioli C, Tagliabue E, Iorio MV, and Croce CM. Oncosuppressive role of p53-induced miR-205 in triple negative breast cancer. *Mol Oncol* 6: 458–472, 2012.
50. Radisky DC, Levy DD, Littlepage LE, Liu H, Nelson CM, Fata JE, Leake D, Godden EL, Albertson DG, Nieto MA, Werb Z, and Bissell MJ. Rac1b and reactive oxygen species mediate MMP-3-induced EMT and genomic instability. *Nature* 436: 123–127, 2005.
51. Semenza GL. Hypoxia-inducible factor 1 (HIF-1) pathway. *Sci STKE* 2007: cm8, 2007.
52. Taylor BS, Schultz N, Hieronymus H, Gopalan A, Xiao Y, Carver BS, Arora VK, Kaushik P, Cerami E, Reva B, Antipin Y, Mitsiades N, Landers T, Dolgalev I, Major JE, Wilson M, Socci ND, Lash AE, Heguy A, Eastham JA, Scher HI, Reuter VE, Scardino PT, Sander C, Sawyers CL, and Gerald WL. Integrative genomic profiling of human prostate cancer. *Cancer Cell* 18: 11–22, 2010.
53. Tlsty TD, and Coussens LM. Tumor stroma and regulation of cancer development. *Annu Rev Pathol* 1: 119–150, 2006.
54. Toullec A, Gerald D, Despouy G, Bourachot B, Cardon M, Lefort S, Richardson M, Rigaill G, Parrini MC, Lucchesi C, Bellanger D, Stern MH, Dubois T, Sastre-Garau X, Delattre O, Vincent-Salomon A, and Mechta-Grigoriou F. Oxidative stress promotes myofibroblast differentiation and tumour spreading. *EMBO Mol Med* 2: 211–230, 2010.
55. Trimmer C, Sotgia F, Whitaker-Menezes D, Balliet RM, Eaton G, Martinez-Outschoorn UE, Pavlides S, Howell A, Iozzo RV, Pestell RG, Scherer PE, Capozza F, and Lisanti MP. Caveolin-1 and mitochondrial SOD2 (MnSOD) function as tumor suppressors in the stromal microenvironment: a new genetically tractable model for human cancer associated fibroblasts. *Cancer Biol Ther* 11: 383–394, 2011.
56. Tryndyak VP, Beland FA, and Pogribny IP. E-cadherin transcriptional down-regulation by epigenetic and microRNA-200 family alterations is related to mesenchymal and drug-resistant phenotypes in human breast cancer cells. *Int J Cancer* 126: 2575–2583, 2010.
57. Tucci P, Agostini M, Grespi F, Markert EK, Terrinoni A, Vousden KH, Muller PA, Dotsch V, Kehrloesser S, Sayan BS, Giaccone G, Lowe SW, Takahashi N, Vandenabeele P, Knight RA, Levine AJ, and Melino G. Loss of p63 and its microRNA-205 target results in enhanced cell migration and metastasis in prostate cancer. *Proc Natl Acad Sci U S A* 109: 15312–15317, 2012.
58. Zheng W, Kuhlicke J, Jackel K, Eltzschig HK, Singh A, Sjoblom M, Riederer B, Weinhold C, Seidler U, Colgan SP, and Karhausen J. Hypoxia inducible factor-1 (HIF-1)-mediated repression of cystic fibrosis transmembrane conductance regulator (CFTR) in the intestinal epithelium. *FASEB J* 23: 204–213, 2009.

Address correspondence to:
Prof. Paola Chiarugi
Department of Biochemical Sciences
University of Florence
Viale Morgagni 50
50134 Firenze
Italy

E-mail: paola.chiarugi@unifi.it

Dr. Nadia Zaffaroni
Department of Experimental Oncology
Fondazione IRCCS Istituto Nazionale dei Tumori
Via Amadeo 42
20133 Milano
Italy

E-mail: nadia.zaffaroni@istitutotumori.mi.it

Date of first submission to ARS Central, March 4, 2013; date of final revised submission, July 26, 2013; date of acceptance, August 6, 2013.

Abbreviations Used

AR = androgen receptor
BCR = biochemical relapse
CAF = cancer-associated fibroblast
CDH1 = E-cadherin
ChIP = chromatin immunoprecipitation
CM = conditioned medium
$CoCl_2$ = cobalt chloride
COX-2 = cycloxygenase-2
DMEM = Dulbecco's modified Eagle's medium
ECM = extracellular matrix
EDTA = ethylene diamine tetraacetic acid
ELISA = enzyme-linked immunosorbent assay
EMT = epithelial-mesenchymal transition
FACS = fluorescence activated cell sorter
FAP = fibroblast activation protein
GEO = Gene Expression Omnibus
GFP = green fluorescent protein
GSEA = gene set enrichment analysis
HIF-1α = hypoxia inducible factor-1α
HPF = human prostate fibroblast
IκB-α = inhibitor of NF-κB
IL-6 = interleukin-6
LNA = locked nucleic acid
MET = mesenchymal-epithelial transition
MIAME = minimum information about a microarray experiment
miRNA = microRNA
MMP = matrix metalloprotease
NaCl = sodium chloride
NF-κB = nuclear factor-κB
PBS = phosphate buffered saline
PCa = prostate cancer
PKCε = protein kinase C epsilon
qRT-PCR = quantitative reverse transcriptase-polymerase chain reaction
ROS = reactive oxygen species
SDS = sodium dodecyl sulfate
TGF-β = tumor growth factor-β
TSS = transcriptional start site

This article has been cited by:

1. Paola Chiarugi, Paolo Paoli, Paolo Cirri. 2014. Tumor Microenvironment and Metabolism in Prostate Cancer. *Seminars in Oncology* **41**, 267-280. [CrossRef]
2. Alessio Cannistraci, Anna Laura Di Pace, Ruggero De Maria, Désirée Bonci. 2014. MicroRNA as New Tools for Prostate Cancer Risk Assessment and Therapeutic Intervention: Results from Clinical Data Set and Patients' Samples. *BioMed Research International* **2014**, 1-17. [CrossRef]
3. Marzia Pennati, Alessia Lopergolo, Valentina Profumo, Michelandrea De Cesare, Stefania Sbarra, Riccardo Valdagni, Nadia Zaffaroni, Paolo Gandellini, Marco Folini. 2013. miR-205 impairs the autophagic flux and enhances cisplatin cytotoxicity in castration-resistant prostate cancer cells. *Biochemical Pharmacology* . [CrossRef]